IEEE Access
Multidisciplinary ⋮ Rapid Review ⋮ Open Access Journal

Received March 21, 2020, accepted March 26, 2020, date of publication March 30, 2020, date of current version April 23, 2020.

Digital Object Identifier 10.1109/ACCESS.2020.2984385

Online Degradation State Assessment Methodology for Multi-Mode Failures of Insulated Gate Bipolar Transistor

XIANGXIANG LIU[1,2], LINGLING LI[1], DIGANTA DAS[2], (Member, IEEE), IJAZ HAIDER NAQVI[2,3], (Member, IEEE), AND MICHAEL G. PECHT[2], (Life Fellow, IEEE)

[1]State Key Laboratory of Reliability and Intelligence of Electrical Equipment, Hebei University of Technology, Tianjin 300000, China
[2]Center for Advanced Life Cycle Engineering (CALCE), University of Maryland, College Park, MD 20742, USA
[3]Department of Electrical Engineering, Lahore University of Management Sciences (LUMS), Lahore 54792, Pakistan

Corresponding author: Lingling Li (lilinglinglaoshi@126.com)

This work was supported in part by the Joint Doctoral Training Foundation of HEBUT, Natural Science Foundation of Hebei Province of China under Grant 2018202282, and in part by the Natural Science Foundation of Tianjin City under grant 19JCZDJC32100.

ABSTRACT Insulated-gate bipolar transistors (IGBTs) are one of the most vulnerable components that account for a significant fraction of inverter and converter failures. This paper conducts a degradation analysis of IGBTs using run-to-failure measurements. Online assessment of the degradation state of IGBTs can prolong normal operation and enable proactive maintenance of the system. The research idea is to find a reliable and robust mechanism for IGBT degradation assessment. This paper developed a prediction interval-based degradation assessment methodology that accurately classifies different health states or degradation levels of IGBTs by adding prediction bounds and using them as a critical value for serious damage. It first computes the prediction interval and then uses the Mahalanobis distance to classify the state into degradation level 1 and degradation level 2, instead of just applying the base algorithm. The developed method outperforms distance-based classification schemes and self-organizing maps for online assessment of degradation levels. It only requires training of 1000 initial points which are assumed to be healthy. Furthermore, the generalizability of the method has been shown by validating the effectiveness of the proposed method on three other modules.

INDEX TERMS IGBT, online degradation state assessment, MD, SOM.

I. INTRODUCTION

Insulated-gate bipolar transistors (IGBTs) are widely used in solar energy, wind energy, electric vehicles, and other energy industries. In power electronics, IGBTs are estimated to be responsible for 34% of all inverter failures, indicating that the reliability of power electronics is highly dependent on the reliability of the IGBT module [1], [2]. It is desirable that the failures of IGBT occur in a fail-safe manner, and an online degradation state assessment helps in reaching that goal.

Several papers have concentrated on physics-of-failure-based and data-driven techniques for early anomaly detection and lifetime prediction of IGBTs. In particular, Valentine *et al.* [3] investigated the physics of failure of metal–oxide–semiconductor field-effect transistors (MOSFETs) and IGBTs and hypothesized that the failures are a combination of manufacturing defects and poor thermal management. Patil *et al.* [4]–[6] tested the degradation performance of IGBT under different stress conditions like temperature. Ghimire *et al.* [7], [8] studied online degradation diagnosis using a single parameter. Patil *et al.* [9]–[14] carried out the diagnostics and prognostics of IGBT by using Mahalanobis distance (MD) of the selected parameters. Sutrisno *et al.* [15] used a k-nearest neighbor algorithm for early anomaly detection. Rigamonti *et al.* [16]–[18] used a self-organizing map (SOM) to cluster different degradation states of the module or different faults of an IGBT in a fully electric vehicle system. Alghassi *et al.* [1] used the k-means method to predict the degradation state of an IGBT module. The accuracy of these methods has not been compared.

The associate editor coordinating the review of this manuscript and approving it for publication was Derek Abbott.

In the process of predicting the degradation state of the module, collector to emitter voltage, $V_{ce,}$ power, P, and case temperature, T_c, or junction temperature, T_j, are the most commonly used features. Amongst these features, collector voltage serves as the primary feature for failure analysis. In addition, since the collector voltage is affected by power and temperature fluctuations, so V_{ce}, P and T_c are selected [7], [20], [21].

The distance-based method and self-organizing map method are very commonly used for anomaly detection or degradation assessment. However, these two methods may give a misleading result when the module experiences more than one degradation stage especially the superposition of multi degradation modes in the later period which may lead to irregular fluctuation in the data.

In this paper, a prediction interval-based methodology for degradation state assessment of IGBTs has been developed based on run-to-failure measurements of multiple IGBTs. The time series raw data of collector voltage and case temperature were used to compute the power. The data were first preprocessed to remove the transients and nonoperational time period and then down-sampled before being labeled using the 3D representation of the preprocessed data. Thereafter, the degradation assessment was conducted using three different methods: i) Mahalanobis distance (MD) based method ii) self-organizing map (SOM), and iii) the developed prediction interval-based classification. The novel method was developed after critically analyzing the MD and SOM methods and their inability to classify the degradation states. The results are compared to determine the accuracy and effectiveness of the methods for the online degradation state assessment. Figure 1 shows the flowchart of the approach that has been followed.

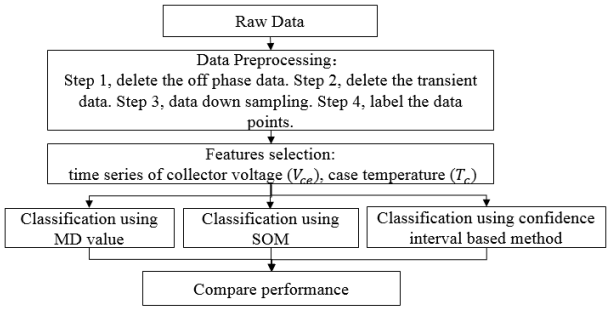

FIGURE 1. Degradation state assessment flowchart.

The rest of the paper is organized as follows. Section II presents the measurement setup, data collection process along with some plots of raw data to infer some key trends and information. Thereafter, Section III discusses the data preprocessing process. In Section IV, the results using distance-based and cluster-based methods are presented and analyzed. Section V explains the prediction interval-based method, presents and analyzes the results on multiple modules to validate the applicability of the developed methodology. Finally, Section VI presents the conclusions.

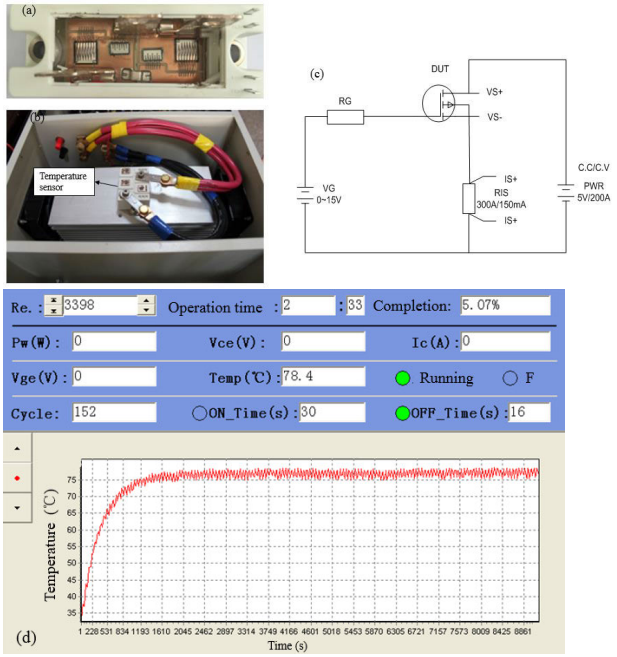

FIGURE 2. Aging device and its circuit.

II. MEASUREMENT SETUP

The measurement setup for the run to failure measurements of IGBT has been shown in Figure 2. The IGBT module (Figure 2a) is installed in an aging chamber shown in Figure 2b and wired using a circuit diagram shown in Figure 2c. The measurements can be controlled from outside of the chamber using a control panel shown in Figure 2d. The IGBT module, also called the device under test (DUT), was powered by two supplies, a program-controlled test power supply (PWR) of 5 V/300 A and a gate-foot program control power supply (VG) of 0–15 V. The gate pin series resistance (RG) of 10 Ω/2 W was used to limit the input current whereas a current transformer (RIS) of 150mA–300 A was used at the source terminal. This is a custom made measurement setup to conduct run to failure measurements. The aging measurements are carried out in two modes, one involves setting the temperature range, and the other involves setting the on-off (duty cycle) time. In both modes, the collector current is set to 50 A whereas the collector voltage of 20 V is used based on the module's datasheet specifications. The gate voltage data is collected once the aging process begins The measurements are stopped at a specified cycle number well beyond the expected life cycle of the module. In the on-off mode, the duty-cycle for is fixed and the temperature is controlled by changing the power. Module A is set to a duty cycle of 50% with an on-time of 30 seconds followed

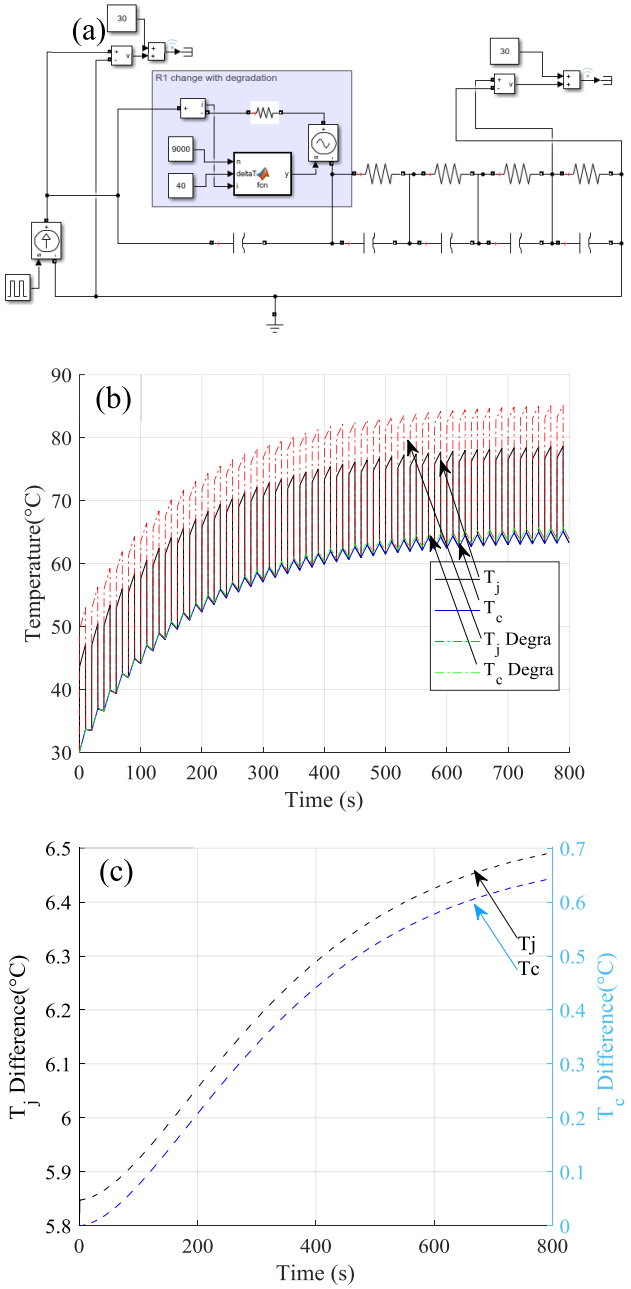

FIGURE 3. Change trend of junction temperature and case temperature.

by 30 s off-time. The duty cycle for module B is also 50% both the on/off times are set to 10 s. The collector voltage decreases to less than 5 V once the circuit is turned on. There is a temperature sensor in contact with the module (between the module and heatsink). Current and voltage measurement wires were connected to the collector, emitter, and gate separately. The run-to-failure measurements (collector voltage, case temperature, and power) for the on-off mode were collected using an aging machine.

In the paper, the case temperature is used to represent the effects of changes in the junction temperature. In order to validate this hypothesis, a simulation model before and after the degradation [22] was built as shown in Figure 3a. The junction to case thermal impedance is estimated using the transient double interface method whereas the case to ambient impedance is estimated by using experimental case temperature data and parameter estimator tool. Simulation results and temperature variations for both case and junction temperature are shown separately in Figure 3b and Figure 3c respectively. The results show that both case and junction temperature demonstrate similar trends before and after degradation as shown in Figure 3c. Therefore, it is reasonable to use the case temperature to represent the effects of changes in the junction temperature.

III. DATA PREPROCESSING

Throughout this paper, we give values for the case temperature and the collector voltage. The power measurements have similar behavior to the collector voltage because of the constant current condition. Figure 4 and Figure 5 show the plots for the measured data after removing the off-phase data. It is observed that the original data did not show anything of significance for the case temperature or collector voltage before and after the removal of the off phase data. Thus, to avoid redundancy and make useful information clear, the original data is not shown here.

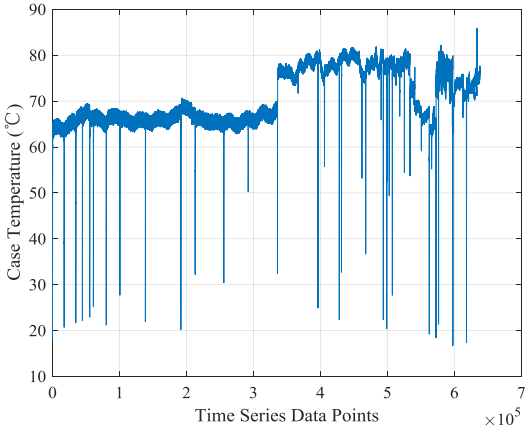

FIGURE 4. Case temperature after removing the off-phase data.

A. REMOVAL OF OFF-PHASE DATA

The first step in data preprocessing is to delete the data where the circuit is switched off (the off-phase data). Figure 4 and Figure 5 show the plots for the measured data after deleting the off-phase data. Since we have deleted the off-phase data, we do not label the x-axis as time, rather we label it ''Time series data points'', which will also be easier to explain the data preprocessing process. Measurements have a sampling interval of 1.6 s. It is important to use the interaction among different parameters to assess the degradation holistically.

Three distinct phases are evident in both these figures. In phase 1, both the case temperature and collector voltage are relatively constant. After 350 K data points, there is a jump in the values but the net trend is still constant.

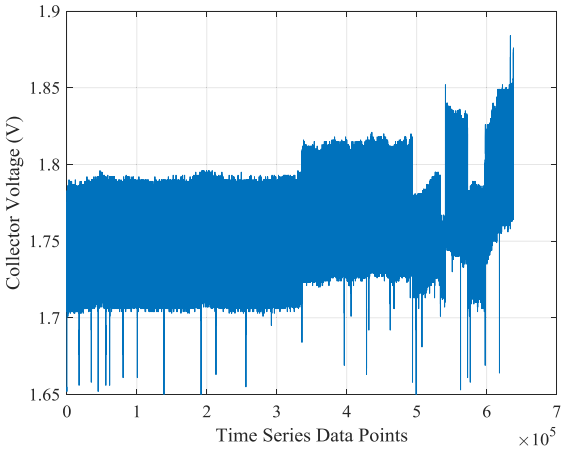

FIGURE 5. Collector voltage after removing the off-phase data.

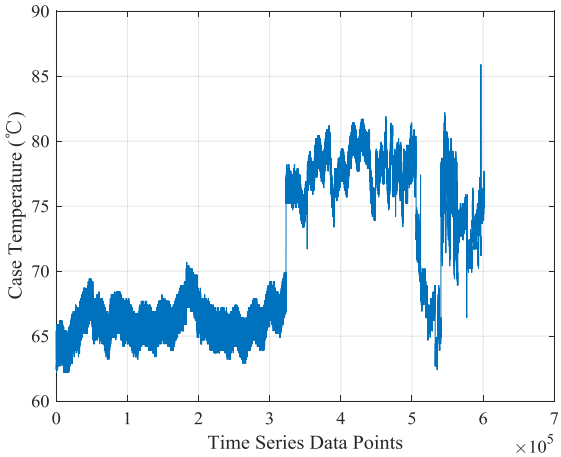

FIGURE 6. Case temperature after removing the transient data.

After 500 K data points, there are some fluctuations in both the case temperature and collector voltage.

B. REMOVAL OF TRANSIENT DATA

In Figure 4, there are large peaks in case temperature that occur every time the aging machine is restarted. The temperature increases rapidly at that phase, it takes several minutes for the case temperature to go from 20°C to 70°C. We refer to these fluctuating data points as transient data points. Transient data points have a temperature increase of more than 5°C between two adjacent points. The transient data points do not represent the degradation of the IGBT and may lead to incorrect conclusions since the initial transient data points may interfere with the stable data points after degradation has occurred as shown in the Figure 8a where a 2-D plot of collector voltage vs the case temperature has been shown without removing the transient data. The transient data takes only 2% of all data, so the removal of the transient data points will not affect the result. Figure 8b shows the same 2-D plot after removing the transient points. It is clear that by removing the transient data, the plots are much cleaner. In this paper, only the data after removing the transient phase is used for health assessment. Figure 6 and Figure 7 show the plots after removing the transient data points.

C. DATA DOWNSAMPLING

Figure 8b shows how the data points are downsampled. It shows four groups of 100 data points along with their average value. The groups are chosen from different regions of the input space: the first group is from the first 100 points, the second group is taken right after 200 K data points, the third group after 400 K data points, and the fourth group after 600 K data points. These samples show interesting patterns. For the first group, the collector voltage increases from 1.72 V to 1.78 V with an average marked with a red circle, and the temperature remains relatively constant. For the second group, the average temperature increases a little. For the third group, the average temperature further increases and this time

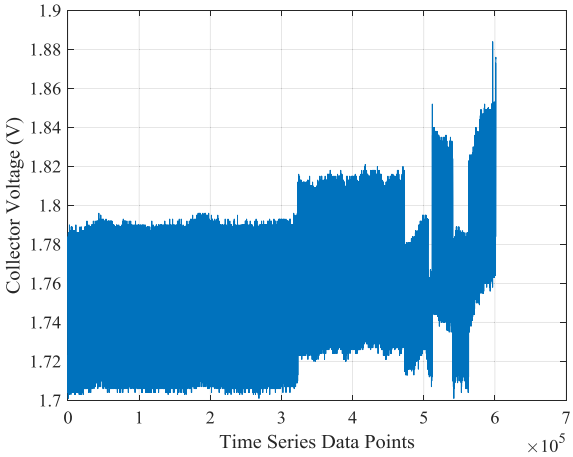

FIGURE 7. Collector voltage after removing the transient data.

by more than 12°C. However, for the fourth group (taken after 600 K data points), the temperature decreases, making a different angle from the start of the process as shown in Figure 8b.

For downsampling different window sizes were considered. For instance, downsampling by taking the average value of 1000 data points or 100 data points showed similar results. In the meantime, using a window size of 100 data points provides data points, which is helpful for the degradation state assessment. For the remainder of the analysis, downsampled data is used. The detail of every step is shown clearly here so that the entire process can be implemented online.

D. DATA LABELING

In order to see the degradation trend of the entire dataset, Figure 9 shows a 3D plot of the data. The downsampled data for collector voltage and case temperature has been plotted with data points (time) increasing in the z-axis direction. As the measurements progress, both case temperature and collector voltage start to increase. At a certain point in time, there is a sudden increase in both parameters. Finally, beyond

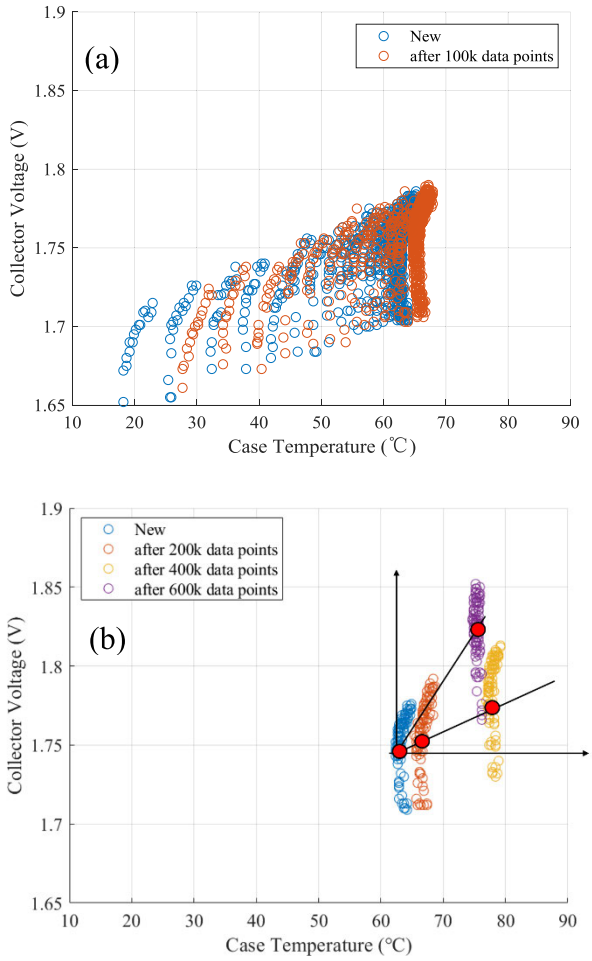

FIGURE 8. Collector voltage vs case temperature before (a) and after (b) removing the transient data. The red dots in (b) show the mean value of the group of data.

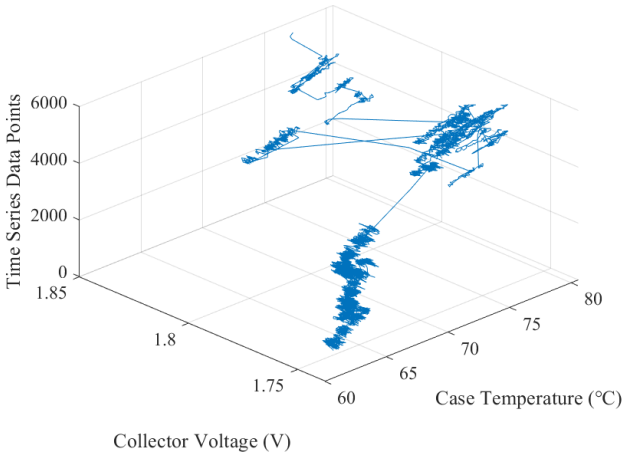

FIGURE 9. Data points change with degradation.

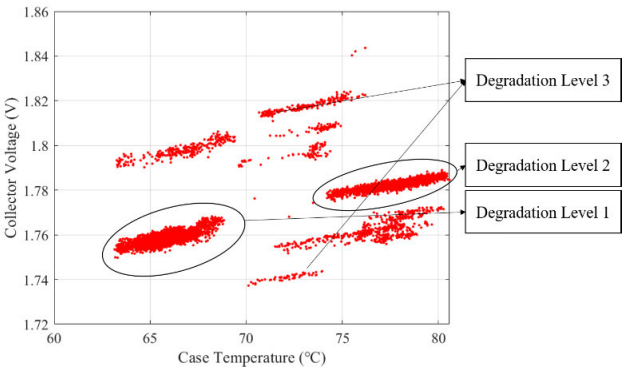

FIGURE 10. Relationship of collector voltage and case temperature.

a certain state, there are rapid fluctuations, with both the case temperature and collector voltage experiencing fluctuations. The 3D figure is used to label the data points into three degradation levels. In order to label the data points, their projection on the *x*-*y* plane is considered and is shown in Figure 10. Three degradation levels can clearly be seen in this figure. The first level consists of a normal and healthy state where a very slight increase is observed in both parameters. Thereafter, degradation level 2 is the state after a sudden increase in both the parameters, but still no rapid fluctuations are observed. This state is a ''degraded state'' but it is still not ''unhealthy''. Finally, after a certain point, rapid fluctuations are observed and are considered as degradation level 3 or the ''unhealthy'' state. The variance of the unhealthy data points is considerably larger than the variance of the first 1000 data points, which are assumed to be healthy. All the labeling is used as a reference in the classification.

IV. DEGRADATION STATE ASSESSMENT

Two methods are commonly used for degradation level assessment—a distance-based method and a clustering-based method. In this Section, these two kinds of methods are discussed, and the performance results with each of these methods are presented and analyzed.

A. DISTANCE-BASED METHOD

Mahalanobis distance (MD) is one of the most commonly used distance metrics. The MD represents the covariance distance between the test data and the reference distribution. It takes into account the relationship between the various features of the reference distribution. It is an effective way to calculate the similarity of two unknown sample sets. The MD of sample x_i is defined in Eq. (1).

$$\mathrm{MD}_i = \sqrt{(x_i - \mu)^T S^{-1} (x_i - \mu)} \tag{1}$$

where x_i is the ith observation, μ is the mean value of the reference data, and S is the covariance matrix of reference data [9]–[14].

Figure 11 shows the MD for all data points. Note that over the course of the run-to-failure measurements, the overall trend of the aging data points is increasing. There is a decrease phase after 5500 data points while the module is in the degraded state. Thus, MD does not represent the degradation of the module accurately. The decrease phase in the MD is the

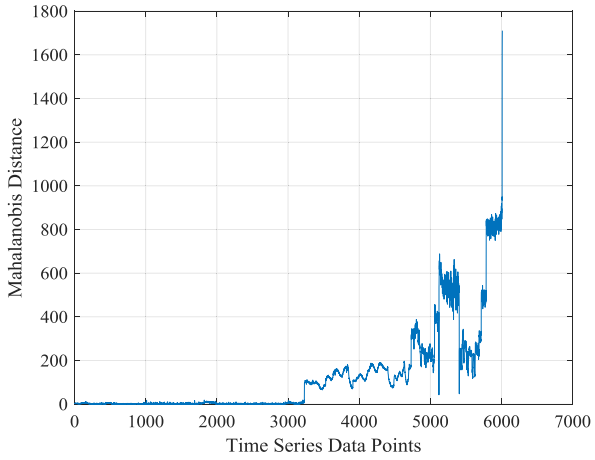

FIGURE 11. Mahalanobis distance of all data points.

degradation level 3 in Figure 10. In degradation level 3, some data points are nearer to the initial (normal) data points than in degradation level 2. Therefore, if the data has this kind of fluctuating trend, the distance-based metric may not work.

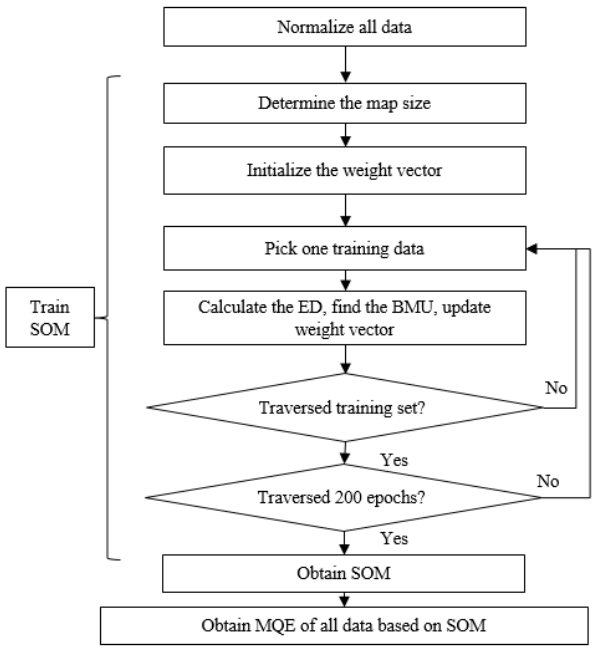

FIGURE 12. Generating a self-organizing map (SOM) and calculating minimum quantization error (MQE).

B. SELF-ORGANIZING MAP

A self-organizing map (SOM) is a type of clustering method that facilitates data visualization by projecting multi-dimensional feature space to a two-dimensional map. A SOM is an unsupervised learning method, it constantly gathers data with similar characteristics through the competition of the neurons to form a two-dimensional map. The entire process of the SOM is shown in Figure 12.

All the data is normalized in the first step. In the second step, the map size, or the number of neurons, is determined by the number of healthy data points, as shown in Eq. (2).

$$M \approx 5\sqrt{N} \tag{2}$$

where M is the number of neurons, usually $\sqrt{M}$ is the length and width of the map, N is the number of health data points. In the third step, the weight vector is initialized by a random number (the weight is a matrix of three rows and M columns). The next five steps iteratively update the weights over 200 iterations to obtain a SOM. The algorithm starts by calculating the Euclidean distance between the first three-dimensional input value and each weight vector. The neuron with the minimum outcome is selected as the best matching unit (BMU) as it is the neuron that is most similar to the input. The weights are mapped to a two-dimensional map of $\sqrt{M}$ by $\sqrt{M}$ where weights are updated depending upon the distance to the BMU. The weights for the i^{th} neuron are then updated using Eq. (3).

$$w_i\,(t+1) = w_i\,(t) + h_{ci}\,(t) \parallel x\,(t) - w_i\,(t) \parallel \tag{3}$$

where $\parallel x\,(t) - w_i\,(t) \parallel$ is the Euclidean distance between $x(t)$ and $w_i(t)$, $h_{ci}(t)$ is the neighborhood function that allows update in the neighborhood of the winning neuron and has a Gaussian distribution as represented in Eq. (4), where $\eta(t)$ (Eq. (5)) is the learning rate and the standard deviation $\sigma(t)$ (Eq. 6) is influenced by radius [16], [23].

$$h_{ci}\,(t) = \eta\,(t) \exp\left(\frac{\parallel r_c - r_i \parallel^2}{2 \times \sigma(\mathrm{t})^2}\right) \tag{4}$$

$$\eta\,(t) = \eta\,(0)\left(\exp\frac{-t}{n}\right) \tag{5}$$

$$\sigma\,(t) = \sigma\,(0) \exp\left(-\frac{t}{\frac{n}{\ln(\sigma\,(0))}})\right) \tag{6}$$

Once the optimal weights are obtained for input, another training data vector is picked up and the process is repeated until optimal weights have been computed for the entire training data and at least 200 iterations have been reached. The process produces a SOM as shown in Figure 13. The SOM clusters data points of different degradation levels together, the blue part is data points that are normal data points, the green part on the right represents degradation level 2, and the yellow part is the data points that are severely damaged (degradation level 3).

Unlike MD, SOM is able to find three clusters from the input. The SOM here is constructed based on all the data points in the aging or run-to-failure measurements. However, practical applications require online degradation assessment. If we want to classify assuming online arrivals, SOM becomes infeasible. For instance, Figure 14 shows the SOM map based on the initial (normal) data points. The observation data points are used as the input of the SOM and the minimum quantization error (MQE) as the output. Even though all the

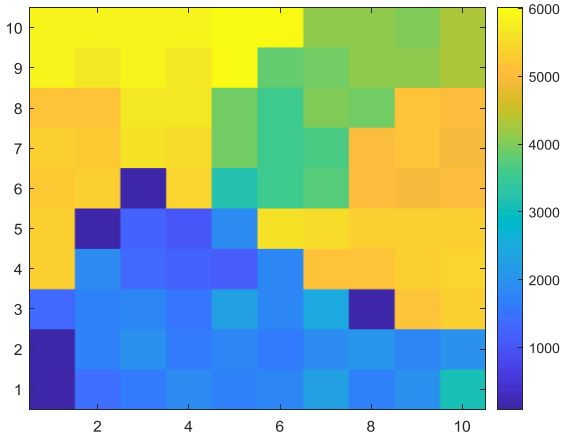

FIGURE 13. Self-organizing map of all data points.

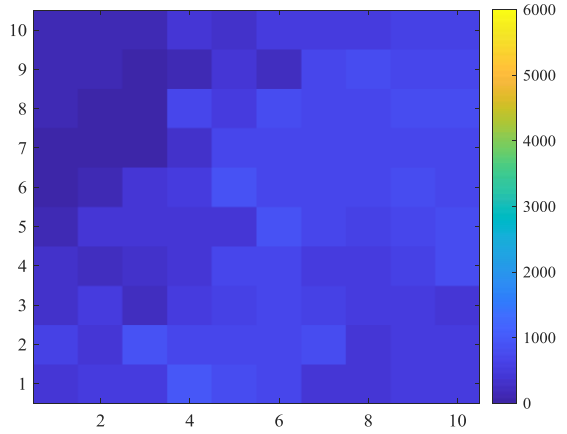

FIGURE 14. Self-organizing map of all data points of 1000 data points.

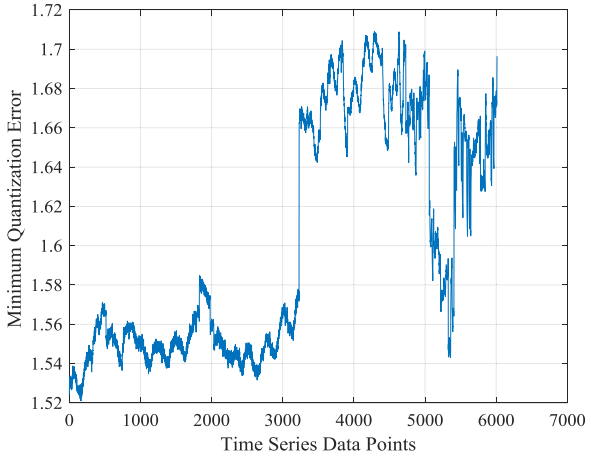

FIGURE 15. Minimum quantization error of all data points.

data points belong to the same class, the SOM still tries to cluster them in different classes and hence assigns incorrect labels to the data points. In fact, the performance is even worse than MD-based classification for the online case. The results are shown in Figure 15.

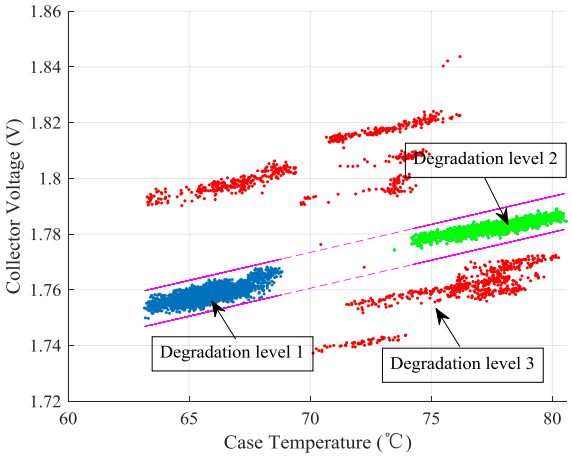

FIGURE 16. Classification by prediction interval-based method.

V. PREDICTION INTERVAL-BASED METHOD

In order to carry out an online degradation assessment, a prediction interval-based method has been developed. A prediction interval is a type of interval estimate, computed from the statistics of the observed data. Factors affecting the width of the prediction interval include the size of the sample, the confidence level, and the variability in the sample.

The prediction interval is based on the existing fit to the data, it accounts for both the uncertainty in estimating the population means and the random variation of the individual values. The equation for calculating the prediction interval is shown in Eq. (7),

$$(\bar{x} - t_b\,(n-1) \times s_{pred}, \bar{x} + t_b\,(n-1) \times s_{pred}) \tag{7}$$

$$s^2_{pred} = s^2 + s^2_{\widehat{y^*}} \tag{8}$$

$$s^2_{\widehat{y^*}} = s^2\left(\frac{1}{n} + \frac{(x^* - \bar{x})}{\Sigma(x_i - \bar{x})^2}\right) \tag{9}$$

where $\bar{x}$ is the sample mean, n is the sample number, $b = \frac{1-C}{2}$, and C is confidence level, critical value $t_b(n-1)$ is computed by searching the Student's t-distribution, s^2 is the variance of the estimation y^*, $s^2_{\widehat{y^*}}$ is the estimated standard deviation of samples, it indicates the variance because of using y^* to estimate $E(y^*)$, x^* is the individual sample, x_i is an ith sample, y^* is the estimated value based on the samples [24].

In this paper, the initial 1000 data points are used as the reference data points, and the prediction bound is drawn based on the prediction interval of 0.9999 to make sure that the bound can cover most of the healthy data. The prediction bound separates data in degradation level 1 and 2 from degradation level 3. When the online test data is within the bound, it is either in degradation level 1 or 2. When 3 consecutive data points of the online test data points exceed the bound, the module is considered to be damaged and hence in degradation level 3. When the test data is within the prediction bound, MD is used to divide the state of the module by a threshold value. The conservative threshold value of $\mu + 12\sigma$ from the first 1000 data points is used to separate degradation

levels 1 and 2. Thus, the data points within the threshold are considered to be healthy data. The data points exceeding the threshold but still within the confidence bounds are regarded as the points in degradation level 2. Finally, the points that are consistently out of the prediction interval are regarded as the points in degradation level 3. In the process, if the module is not in the unstable state but the case temperature value keeps on increasing in degradation level 2 and exceeds 150% of the mean value of the original 1000 data points, it will also be classified as degradation level 3.

To show how degradation levels 1 and 2 can be separated from level 3, the absolute value of the difference from the mean value is plotted in Figure 17. The threshold is based on the confidence bound that ensures that 99.99% of the first 1000 data points are within the bounds. When three consecutive data points are over the threshold, they lie in degradation level 3. Please note that each point here is the mean of 100 data points. The number three has been arbitrarily chosen. Three consecutive data points are selected to avoid possible misjudgment it is a fairly conservative judgment where the impact three hundred data points are considered before making a declaration, and once it is classified as degradation level 3, it won't be classified as level 2.

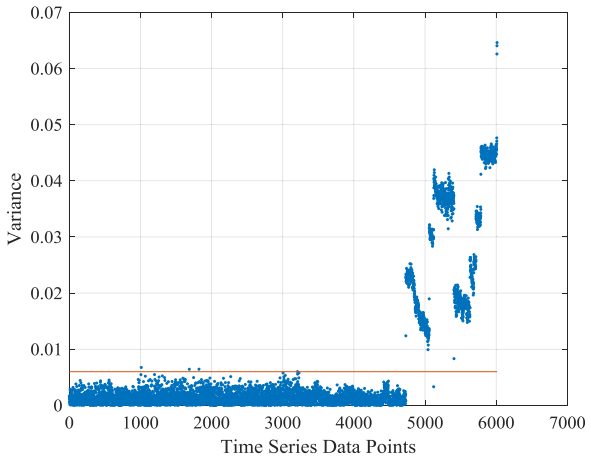

FIGURE 17. Variance of all data points to the middle line.

Figure 17 clearly demonstrates that this approach can easily separate degradation level 3 from degradation levels 1 and 2. To distinguish degradation level 2 from level 1, MD is used, the result is shown in Figure 18. It can be seen that the data starts in degradation level 1 and moves to degradation level 2 after around 3100 data points. The degradation assessment of the prediction interval method can be realized in an online manner.

To verify the effectiveness of the developed method, the run-to-failure measurements of another IGBT (module B) were carried out, as shown in Figure 19. This module hardly experienced degradation level 2 and jumped directly from the degradation level 1 to level 3. This result proves the effectiveness of the prediction interval-based degradation classification. The method achieved a classification accuracy

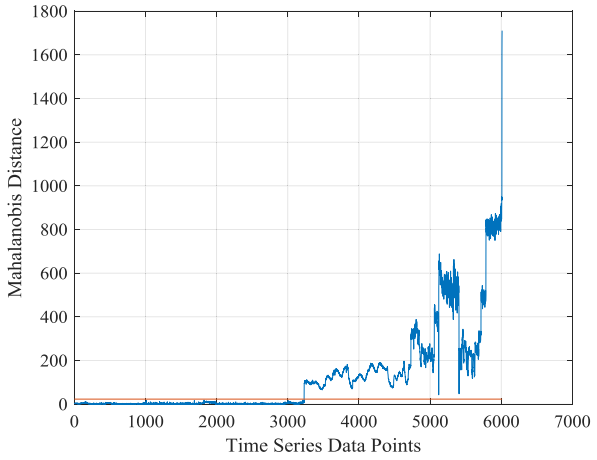

FIGURE 18. Mahalanobis distance threshold for distinguishing degradation levels 1 and 2.

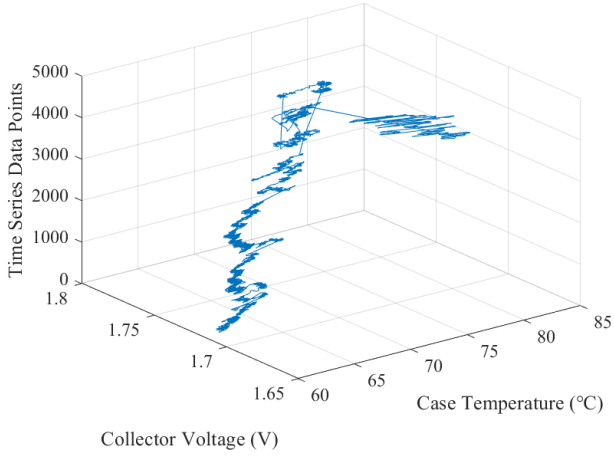

FIGURE 19. Data points change with the degradation of module B.

of 98.4% when it classified 76 data points in degradation level 3 instead of level 1. However, all those data points were just before the module reached degradation level 3 as shown in Figure 20. Some red data points in the prediction bound are misclassified, but it only accounts for less than 2% of the total points. This validates the applicability of the developed method across different modules.

To demonstrate the generalizability of the method, additional modules that work under different aging modes are used to validate the methodology. As mentioned in Section II, there are two aging modes; one uses the temperature range and the other sets the on-off time. The temperature range for the aging of module C is set to 40°C -90°C whereas temperature range settings for the aging of module D is set to 30°C -70°C.

The time-series data points distribution and the prediction interval results for module C are shown separately in Figure 21a and Figure 21b.

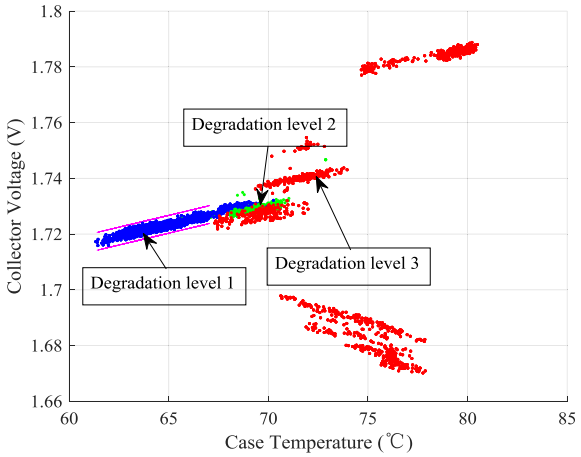

FIGURE 20. Classification by prediction interval-based method of module B.

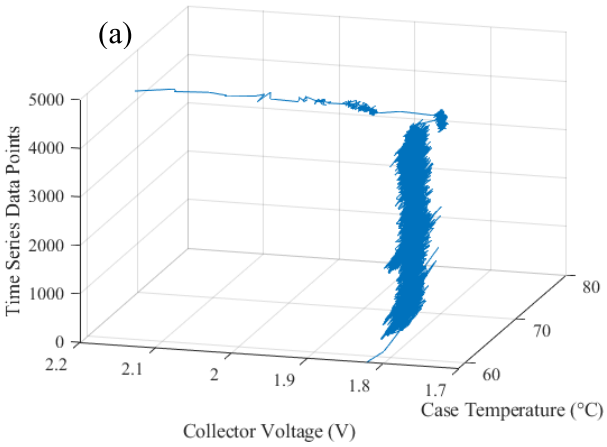

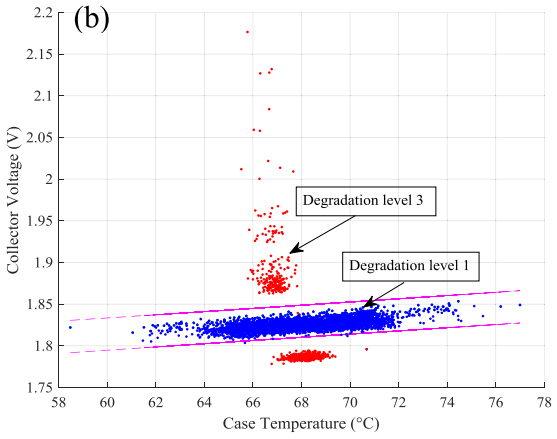

FIGURE 21. Time series data points distribution and classification by prediction interval-based method of module C.

The time-series data points distribution and the prediction interval results for module D are shown separately in Figure 22a and Figure 22b.

The results show that the prediction interval method worked well for both modules C and module D, where the degraded state was effectively detected using the prediction

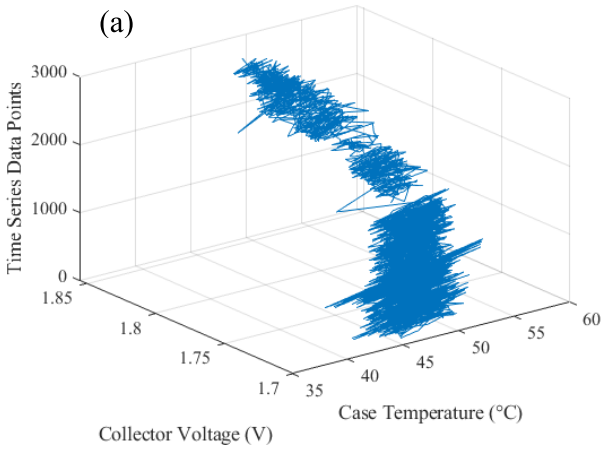

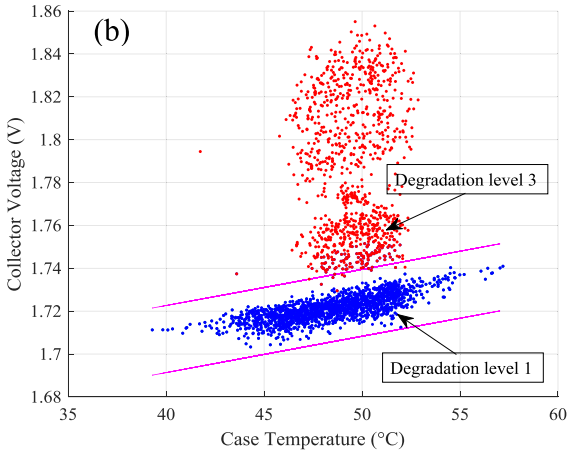

FIGURE 22. Time series data points distribution and classification by prediction interval-based method of module D.

interval method. However, unlike modules A and B, neither of them experienced the degradation level 2, they directly moved from a healthy state to an unhealthy state shortly before they stopped working. Distance-based methods or self-organizing map-based method are not suitable for such variations in the data as they are more effective for the data with a little variance whereas the proposed methodology not only works well for the module that experiences three degradation levels but also for modules where it directly moves to degradation level three from healthy state.

In addition, the change in ambient temperature impacts both the case temperature and voltages and does not affect the degradation assessment.

VI. CONCLUSION

This paper developed a prediction interval-based classification methodology for the degradation state assessment of IGBT modules. First, we showed that Mahalanobis distance (MD) and self-organizing maps (SOMs) are not suitable for degradation assessment of IGBT modules in an online manner. Mahalanobis distance-based classification is not suitable because of the fluctuations of features such as collector voltage and temperature as the module gets

degraded. Self-organizing maps are suitable for clustering the data points with similar features when all the data points are available. Online classification requires a large amount of training data, which may not be suitable for practical applications. The results of online degradation assessment using self-organizing maps and minimum quantization error (MQE) of all data points were no better than the Mahalanobis distance results.

The developed prediction interval-based method outperforms the self-organizing map and Mahalanobis distance methods for online data degradation assessment. The method classifies the data points into three degradation levels in an online manner and does not require a large number of data points (the initial 1000 points in the healthy state) for training. Furthermore, the prediction interval-based method can be extended to other modules with more than 98% accuracy.

The prediction interval-based method takes data space distribution into consideration in comparison to the distance-based methods (not only Mahalanobis distance) that is only suitable for data with two degradation states and may result in the replacement of modules earlier than required. The Mahalanobis distance method is based on the distribution of health data and uses the MD as an indicator. The MD results could be misleading when the measurement data fluctuates in cases where there are multiple degradation modes. The self-organizing map was not as good as MD based classification when it was applied for online degradation assessment.

The work in the paper was carried out under experimental conditions. For further work, real working conditions will be considered. For real application situations, a simulation model will be built that takes the real power signal and ambient temperature as the input and outputs case temperature and collector voltage. The simulation results will be obtained and compared with the experimental results to obtain the degradation assessment.

REFERENCES

[1] A. Benmansour, S. Azzopardi, J. C. Martin, and E. Woirgard, "A step by step methodology to analyze the IGBT failure mechanisms under short circuit and turn-off inductive conditions using 2D physically based device simulation," *Microelectron. Reliab.*, vol. 47, nos. 9–11, pp. 1800–1805, 2007.

[2] J. L. Hudgins, "Power electronic devices in the future," *IEEE J. Emerg. Sel. Topics Power Electron.*, vol. 1, no. 1, pp. 11–17, Mar. 2013, doi: 10.1109/JESTPE.2013.2260594.

[3] N. Valentine, D. Das, B. Sood, and M. Pecht, "Failure analyses of modern power semiconductor switching devices," in *Proc. Int. Symp. Microelectron.*, Oct. 2015, pp. 000690–000695, doi: 10.4071/isom-2015-tha56.

[4] N. Patil, S. Menon, D. Das, and M. Pecht, "Anomaly detection of non punch through insulated gate bipolar transistors (IGBT) by robust covariance estimation techniques," in *Proc. 2nd Int. Conf. Rel., Saf. Hazard-Risk-Based Technol. Phys. Failure Methods (ICRESH)*, Dec. 2010, pp. 68–72, doi: 10.1109/ICRESH.2010.5779635.

[5] N. Patil, D. Das, K. Goebel, and M. Pecht, "Identification of failure precursor parameters for insulated gate bipolar transistors (IGBTs)," in *Proc. Int. Conf. Prognostics Health Manage.*, Oct. 2008, pp. 1–5, doi: 10.1109/PHM.2008.4711417.

[6] N. Patil, D. Das, C. Yin, H. Lu, C. Bailey, and M. Pecht, "A fusion approach to IGBT power module prognostics," in *Proc. 10th Int. Conf. Thermal, Mech. Multi-Phys. Simul. Exp. Microelectron. Microsyst. (EuroSimE)*, Apr. 2009, pp. 1–5, doi: 10.1109/ESIME.2009.4938491.

[7] P. Ghimire, S. Beczkowski, S. Munk-Nielsen, B. Rannestad, and P. B. Thøgersen, "A review on real time physical measurement techniques and their attempt to predict wear-out status of IGBT," in *Proc. 15th Eur. Conf. Power Electron. Appl. (EPE)*, Lille, France, 2013, doi: 10.1109/EPE.2013.6634419.

[8] S. Beczkowski, P. Ghimre, A. R. de Vega, S. Munk-Nielsen, B. Rannestad, and P. Thogersen, "Online VCE measurement method for wear-out monitoring of high power IGBT modules," in *Proc. 15th Eur. Conf. Power Electron. Appl. (EPE)*, Lille, France, Sep. 2013, pp. 1–7, doi: 10.1109/EPE.2013.6634390.

[9] N. Patil, J. Celaya, D. Das, K. Goebel, and M. Pecht, "Precursor parameter identification for insulated gate bipolar transistor (IGBT) prognostics," *IEEE Trans. Rel.*, vol. 58, no. 2, pp. 271–276, Jun. 2009, doi: 10.1109/TR.2009.2020134.

[10] N. Patil, D. Das, and M. Pecht, "Anomaly detection for IGBTs using Mahalanobis distance," *Microelectron. Rel.*, vol. 55, no. 7, pp. 1054–1059, Jun. 2015, doi: 10.1016/j.microrel.2015.04.001.

[11] N. Patil, D. Das, and M. Pecht, "A prognostic approach for non-punch through and field stop IGBTs," *Microelectron. Rel.*, vol. 52, no. 3, pp. 482–488, Mar. 2012, doi: 10.1016/j.microrel.2011.10.017.

[12] M. Pecht and M. Kang, "Machine learning: Diagnostics and prognostics," in *Prognostics and Health Management of Electronics: Fundamentals, Machine Learning, and Internet of Things*. Piscataway, NJ, USA: IEEE Press, 2019, pp. 170–181.

[13] N. Patil, D. Das, and M. Pecht, "Mahalanobis distance approach for insulated gate bipolar transistors (IGBT) diagnostics," in *New World Situation: New Directions in Concurrent Engineering* (Advanced Concurrent Engineering). London, U.K.: Springer, Nov. 2010, pp. 583–591, dio: 10.1007/978-0-85729-024-3_60.

[14] N. Patil, S. Menon, D. Das, and M. Pecht, "Evaluation of robust covariance estimation techniques for anomaly detection of insulated gate bipolar transistors (IGBT)," in *Proc. ASME Conf. Smart Mater., Adapt. Struct. Intell. Syst.*, Jan. 2010, pp. 769–773, doi: 10.1115/smasis2010-3861.

[15] E. Sutrisno, Q. Fan, D. Das, and M. Pecht, "Anomaly detection for insulated gate bipolar transistor (IGBT) under power cycling using principal component analysis and K-nearest neighbor algorithm," *J. Washington Acad. Sci.*, vol. 98, no. 1, pp. 1–8, 2012.

[16] M. Rigamonti, P. Baraldi, A. Alessi, E. Zio, D. Astigarraga, and A. Galarza, "An ensemble of component-based and population-based self-organizing maps for the identification of the degradation state of insulated-gate bipolar transistors," *IEEE Trans. Rel.*, vol. 67, no. 3, pp. 1304–1313, Sep. 2018, doi: 10.1109/TR.2018.2834828.

[17] M. Rigamonti, P. Baraldi, E. Zio, A. Alessi, D. Astigarraga, and A. Galarza, "Identification of the degradation state for condition-based maintenance of insulated gate bipolar transistors: A self-organizing map approach," *Microelectron. Rel.*, vol. 60, pp. 48–61, May 2016, doi: 10.1016/j.microrel.2016.02.015.

[18] M. Rigamonti, P. Baraldi, E. Zio, A. Alessi, D. Astigarraga, and A. Galarza, "A self-organizing map-based monitoring system for insulated gate bipolar transistors operating in fully electric vehicle," in *Proc. Annu. Conf. Progn. Heal. Manag. Soc. (PHM)*, 2015, pp. 253–261.

[19] A. Alghassi, S. Perinpanayagam, and I. K. Jennions, "A simple state-based prognostic model for predicting remaining useful life of IGBT power module," in *Proc. 15th Eur. Conf. Power Electron. Appl. (EPE)*, Sep. 2013, pp. 1–7, doi: 10.1109/EPE.2013.6634482.

[20] N. Patil, "Prognostics of insulated gate bipolar transistors," Ph.D. dissertation, Dept. Macha. Eng., Univ Maryland, College Park, MD, USA, 2011.

[21] I. Hirano, Y. Nakasaki, S. Fukatsu, M. Goto, K. Nagatomo, S. Inumiya, K. Sekine, Y. Mitani, and K. Yamabe, "Time-dependent dielectric breakdown (TDDB) distribution in n-MOSFET with HfSiON gate dielectrics under DC and AC stressing," *Microelectron. Rel.*, vol. 53, no. 12, pp. 1868–1874, Dec. 2013, doi: 10.1016/j.microrel.2013.05.010.

[22] X. Liu, L. Li, D. Das, and M. Pecht, "Microelectronics reliability an electro-thermal parametric degradation model of insulated gate bipolar transistor modules," *Microelectron. Reliab.*, vol. 104, 2020, Art. no. 113559, doi: 10.1016/j.microrel.2019.113559.

[23] J. Tian, M. Azarian, and M. Pecht, "Anomaly detection using self-organizing maps-based k-nearest neighbor algorithm," in *Proc. Eur. Conf. Prognostics Health Manage. Soc.*, 2014. [Online]. Available: https://pdfs.semanticscholar.org/0cfc/ffcf796f0f2f2be202222a07584c947454 1c.pdf

[24] M. Jørgensen and D. I. K. Sjøberg, "An effort prediction interval approach based on the empirical distribution of previous estimation accuracy," *Inf. Softw. Technol.*, vol. 45, no. 3, pp. 123–136, Mar. 2003, doi: 10.1016/S0950-5849(02)00188-X.

XIANGXIANG LIU was born in Hebei, China, in 1991. She received the B.S. and M.S. degrees in electrical engineering from the Hebei University of Technology, Tianjin, China, in 2013 and 2016, where she is currently pursuing the Ph.D. degree in electrical engineering. From 2017 to 2019, she was a Visiting Student with the Center for Advanced Life Cycle Engineering (CALCE), University of Maryland, USA. Her main research include online monitoring and anomaly detection of semiconductor, and prognostic and health management of power systems.

LINGLING LI received the B.S. degree in industrial process measurement and control instrument from Tianjin University, Tianjin, China, in 1989, and the M.S. degree in control theory and control engineering and the Ph.D. degree in electric machines and electric apparatus from the Hebei University of Technology, Tianjin, in 2001 and 2004, respectively.

Since 2006, she has been a Professor with the School of Electrical Engineering, Hebei University of Technology. From 2009 to 2012, she was an Electrical Engineering Postdoctoral with Tianjin University. Since 2012, she has also been a Ph.D. Supervisor with the School of Electrical Engineering, Hebei University of Technology. From 2014 to 2015, she was a Visiting Scholar with Northeastern University, Shenyang, China. From 2015 to 2018, she was the Director with Reliability Engineering Branch of China Mechanical Engineering Society, Beijing, China. From 2016 to 2017, she was a Visiting Professor with the National Chin-Yi University of Technology, Taichung City, China. She is the author of more than 100 articles, including more than ten SCI articles. Her research interests include reliability of electrical apparatus, power systems, and new energy.

DIGANTA DAS (Member, IEEE) received the B.Tech. degree in manufacturing science and engineering from the Indian Institute of Technology Kharagpur, Kharagpur, India, and the Ph.D. degree in mechanical engineering from the University of Maryland, College Park. He is currently a Member of the Research Staff with the Center for Advanced Life Cycle Engineering (CALCE), University of Maryland. His expertise is in reliability, environmental, and operational ratings of electronic parts, uprating, electronic part reprocessing, counterfeit electronics, technology trends in the electronic parts and parts selection, and management methodologies. He performs benchmarking processes and organizations of electronics companies for parts selection and management and reliability practices. He has published more than 60 articles on these subjects and presented his research at international conferences and workshops. He is an editorial board member of the journal *Microelectronics Reliability* and *Circuit World*. His current research interests include counterfeit electronics avoidance and detection, light-emitting-diode failure mechanisms, cooling systems in telecommunications infrastructure and their impact on reliability, and power electronics reliability. Dr. Das is a Six Sigma Black Belt and a member of IMAPS and SMTA. He is also the Vice Chair of the standards group of the IEEE Reliability Society. He had been the Technical Editor of two IEEE standards. He leads the Educational Outreach of CALCE with responsibility to develop interorganizational agreements on joint educational programs, training and internship program, and professional development.

IJAZ HAIDER NAQVI (Member, IEEE) received the B.Sc. degree in electrical engineering from the University of Engineering and Technology Lahore, Pakistan, in 2003, the master's degree in radio communications from SUPELEC Paris, France, in 2006,and the Ph.D. degree in electronics and telecommunications from IETR-INSA Rennes, France, in 2009. He is currently an Associate Professor with the School of Science and Engineering, Lahore University of Management Sciences (LUMS), Pakistan. He has published several refereed articles in international journals and peer-reviewed international conferences. He received several years of research experience in the wireless communications and wireless sensor networks. His current research focuses on 5G networks and beyond, including system level aspects in wireless networks, millimeter wave wireless systems for 5G and 6G telecommunication, and multiantenna radar systems for civilian applications. He also works in the area of reliability engineering investigating degradation and ageing of electronics specially Li-ion batteries.

MICHAEL G. PECHT (Life Fellow, IEEE) received the B.S. degree in physics, the M.S. degree in electrical engineering, and the M.S. and Ph.D. degrees in engineering mechanics from the University of Wisconsin at Madison. He is currently a World-Renowned Expert in strategic planning, design, test, and risk assessment of information systems. He is also the Chair Professor of mechanical engineering and a Professor of applied mathematics with the University of Maryland. He has served on three NAS studies, two U.S. Congressional investigations in automotive safety, and as an Expert for the FDA. He is the Founder and the Director of the Center for Advanced Life Cycle Engineering, University of Maryland, which is funded by over 150 of the world's leading electronics companies at over U.S. six months/years. He is also a Professional Engineer and a Fellow of ASME, SAE, and IMAPS. He received the NSF Innovation Award, in 2009, and the National Defense Industries Association Award. In 2015, he received the IEEE Components, Packaging, and Manufacturing Award for Visionary Leadership in the development of physics-of-failure-based and prognostics-based approaches to electronic packaging reliability. He received the Distinguished Chinese Academy of Sciences President's International Fellowship. In 2013, he received the University of Wisconsin-Madison's College of Engineering Distinguished Achievement Award. In 2011, he received the University of Maryland's Innovation Award for his new concepts in risk management. In 2010, he received the IEEE Exceptional Technical Achievement Award for his innovations in the area of prognostics and systems health management. In 2008, he was a recipient of the highest reliability honor, the IEEE Reliability Society's Lifetime Achievement Award. He is also the Editor-in-Chief of IEEE Access. He has served as a Chief Editor for the IEEE Transactions on Reliability for nine years and the Microelectronics Reliability for 16 years.